Proceedings of the ASME 2015 International Design Engineering Technical Conferences & Computers and Information in Engineering Conference
IDETC/CIE 2015
August 2-5, 2015, Boston, Massachusetts, USA

DETC2015-46241

A LASER CALIBRATION DEVICE FOR MINI ROBOTS

Giovanni Legnani
Department of Mechanical and Industrial Engineering
University of Brescia
Brescia, Italy
Email: giovanni.legnani@unibs.it

Andrea Gabrielli
Department of Mechanical and Industrial Engineering
University of Brescia
Brescia, Italy
Email: andrea.gabrielli@unibs.it

Abdelmajid Ousdad
Department of Mechanical and Industrial Engineering
University of Brescia
Brescia, Italy
Email: a.ousdad@unibs.it

Irene Fassi
Institute of Industrial Technologies and Automation
National Research Council
Milan, Italy
Email: irene.fassi@itia.cnr.it

Serena Ruggeri
Institute of Industrial Technologies and Automation
National Research Council
Milan, Italy
Email: serena.ruggeri@itia.cnr.it

Gianmauro Fontana
Institute of Industrial Technologies and Automation
National Research Council
Milan, Italy
Email: gianmauro.fontana@cnr.it

ABSTRACT

The paper describes a new laser device conceived for surface scanning and more specifically for mini robot calibrations. The system is based on a laser triangulation sensor which is moved by an extremely accurate device to collect a set of 3D points lying on surfaces. If the surfaces belong to the gripper of a robot that must be calibrated and a sufficient number of points of this gripper are collected, the pose of the robot can be measured. If the robot is moved to several different configurations and the gripper poses are measured for each of them, it is possible to reconstruct the kinematics of the robot and calibrate it. The paper presents the theory and describes the design, tests and calibration of the laser instrumentation with a focus on the first experimental results. These results are obtained in a working cell including a vision system, a 4-dof (xyz,θ) mini robot and a 2-dof rotating platform.

INTRODUCTION

Nowadays the increasing pace of technology development due to a request of competitiveness that doesn't show any sign of slowing is affecting every industrial sector; in this direction the possibility to increase the production and reduce the costs is without any doubt charming for every business and is rapidly pushing every industrial context to automate its production processes. The automation of the lines is possible only if the devices hosted inside the workcells can interact without risk of interfering with each other. This is possible only if every single machine is described by a sufficiently accurate kinematic model and can operate in highly structured environments, where a preliminary topological characterization of the space together with the presence of appropriate onboard sensors guarantee the cooperation of the elements without collisions.

One way to increase accuracy, as defined in the international standard ISO 9283 [1], is by kinematic calibration. Since calibration requires effort and cost, it is performed only when strictly necessary. In fact, a general kinematic calibration for robots requires a set of experimental measurements, a suitable measuring system and an appropriate mathematical model [2, 3]. Sometimes calibration has to be based on non-conventional procedures like neural networks [4]. In addition, the experimental measurement of the gripper pose, which is an unavoidable part of the calibration, generally requires high cost sensors. For this reason, the search for practical and low cost measuring devices is still an open issue and in many cases the solutions found are customized for specific applications [5, 6].

The objective of this work is to describe the steps followed in designing and developing an innovative low-budget laser calibration system, useful in tasks that need the identification of points lying on a surface. The system can be used to perform the calibration of every mechanical device, although its dimensions make it more suitable in contexts where the lack of space is a real problem, i.e. in the calibration of mini robotic mechanisms.

Copyright © 2015 by ASME

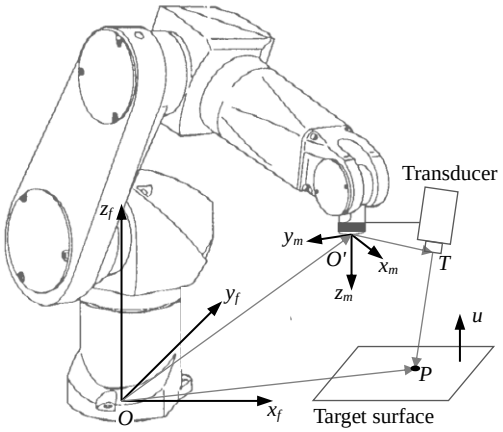

Figure 1. LAYOUT OF THE CALIBRATION SYSTEM.

In fact the system, being lightweight and small size, can be used in small workcells, i.e. volumes of about 0.5 m^3, and perform very accurate assembly tasks with errors around 0.01 mm.

More in detail, if it is possible to identify a point cloud by scanning an object with respect to a fixed reference system, it is also possible to determine its shape, dimensions, position and orientation, as several industrial applications can prove [7, 8]. This is what the reverse engineering technologies are meant to carry out.

Moreover, if the object under scanning is a tool mounted on the end-effector of a robot, the identification of its poses for different robot configurations makes it possible to calibrate the robot itself and identify its actual kinematics.

The work here presented describes how the theory just mentioned has been considered while designing an innovative measuring system. The proposed measuring system consists of a manipulator having at least 4 degrees of freedom (3 for the translation and 1 for the rotation) and a transducer mounted on the same manipulator and able to measure the displacements of a cloud of points lying on a surface. In fact, with reference to Fig. 1, if the position of the transducer is known with respect to the reference system of the robot, when the transducer measures the distance T-P of the target, the absolute position of the point P can be determined. Generally speaking, the identification of the pose of the measuring system with respect to the robot gripper (hand-to-sensor-calibration) requires the solution of a matrix equation in the form AX=XB [9, 10, 11]. In this paper we will develop a more easy, but precise, alternative solution which works in some specific contexts.

The research, conducted in the framework of the project PRIN2009 MM&A, funded by MIUR, has been carried out exploiting the instrumentation available in a workcell designed for the manipulation and assembly of micro-scale sized components [12, 13].

In particular, an already calibrated 4-dof 5-joint closed link robot with Schönflies motion [14] has been used to move a commercial high accuracy laser triangulation sensor and collect the points. The work described in this paper consists in precisely identifying the position and orientation of the laser sensor with respect to the robot gripper and this activity is called "calibration".

In the following sections, first the mathematical model used for the calibration of the device is described. Then the layout of the workcell where the scanning system is meant to work is outlined and a few words are spent to explain the reasons of some design choices. Lastly, the setup of the experiments and the results obtained are reported and in detail described.

SCANNING SYSTEM: MATHEMATICAL MODEL FOR THE CALIBRATION

The scanning system is conceived for being a new and innovative instrument for the identification of the objects position inside a workspace and more specifically for the calibration of robotic devices.

The system is composed of an already calibrated robot with at least 4 degrees of freedom (3 for the translation and 1 for the orientation) and a laser transducer able to measure, along a specific axis, the distance between an inner reference frame and a physical point on a surface. The transducer is mounted on the end-effector of the robot.

To perform the calibration of the system (i.e determining the pose of the sensor with respect to the robot end-effector reference frame) an object of known shape and size must be available; in our case we made use of a flat plane. Then an already calibrated system able to measure the coordinates *x* and *y* of the spot is also necessary; for this purpose we used the vision system described in [15].

The steps are as follows. The robot is moved to a set of 1,2,..*i*,..*n* different poses. For each of these poses the end-effector coordinates $x_{O_i'}$, $y_{O_i'}$, $z_{O_i'}$, and θ_i (rotation around a generic axis) are recorded together with the distance d_i and the coordinates x_{P_i} and y_{P_i} of the spot are measured by the vision system. The data are then processed, taking into account that all the spots lie on a plane whose equation is

$$z = \alpha x + \beta y + \delta \tag{1}$$

with the constants α, β, δ that are unknown and will be determined by the calibration process.

In this case, the unit vector *u*, perpendicular to the plane, can be written as follows.

$$u = \frac{u'}{|u'|} \qquad \text{where} \qquad u' = \begin{bmatrix} \alpha \\ \beta \\ 1 \end{bmatrix} \tag{2}$$

To have a good conditioning of the procedure, the required set of points must contain data collected with different coordinates $x_{O_i'}$, $y_{O_i'}$, $z_{O_i'}$, and θ_i. In this specific case a few

Copyright © 2015 by ASME

planes have been selected, with different coordinate z (a minimum of two planes is required), and in one of them several rotation angles have been used.

A summary of the notation follows. The position of a point P (the laser spot) in the end-effector reference frame can be written as:

$$\overline{O'P}^{O'} = \begin{bmatrix} x_T + a \cdot d \\ y_T + b \cdot d \\ z_T + c \cdot d \end{bmatrix} \tag{3}$$

where x_T, y_T and z_T are the coordinates of a generic point T on the transducer direction with respect to the robot end-effector reference frame O'-$x_m y_m z_m$, d is the distance $|P\text{-}T|$ measured by the transducer, a, b, c are the cosines of the unit vector directed as $\overline{TP}$.

Moreover, the vector of the coordinates of the generic point P in the robot fixed reference frame O-$x_f y_f z_f$ is obtained multiplying the transformation matrix of the robot by the vector of the point coordinates in the end-effector reference frame:

$$\overline{OP}^{O} = \begin{bmatrix} R & \overline{OO'}^{O} \\ 0 & 1 \end{bmatrix} \cdot \overline{O'P}^{O'} \tag{4}$$

where R is the rotation matrix expressing the orientation of the end-effector frame with respect to the absolute frame, while the column vectors $\overline{OP}^{O} = [x_P; y_P; z_P]^O$ and $\overline{OO'}^{O} = [x_{O'}; y_{O'}; z_{O'}]^O$ are respectively the absolute position of P and of the origin of the end-effector frame with respect to the absolute system.

From equation (4) it is possible to obtain:

$$\overline{OP}^{O} - \overline{OO'}^{O} = \begin{bmatrix} x_P - x_{O'} \\ y_P - y_{O'} \\ z_P - z_{O'} \end{bmatrix}^O = R \cdot \begin{bmatrix} x_T + a \cdot d \\ y_T + b \cdot d \\ z_T + c \cdot d \end{bmatrix}^{O'} \tag{5}$$

Following (5), a new matrix $\overline{R}$, is introduced which contains the rotation matrix R alone and multiplied by d:

$$\overline{R} = [R \mid d \cdot R] \tag{6}$$

By remembering that the laser spot lies on the plane (1) and considering (5) and (6) for each experimental point i, we get

$$S_i = \begin{bmatrix} x_{P_i} - x_{O'_i} \\ y_{P_i} - y_{O'_i} \\ -z_{O'_i} \end{bmatrix}^O = \overline{\overline{R}}_i \cdot \begin{bmatrix} x_T^{O'} \\ y_T^{O'} \\ z_T^{O'} - \delta \\ a \\ b \\ c \\ \alpha \\ \beta \end{bmatrix} \tag{7}$$

where i takes the values from 1 to n (the number of the experimental points) and $S_i = [x_{P_i} - x_{O'_i}; y_{P_i} - y_{O'_i}; -z_{O'_i}]^O$.

Combining the n $\overline{\overline{R}}_i$ and the n S_i matrixes together in $\overline{\overline{R}} = \begin{bmatrix} \overline{\overline{R}}_1^T .. \overline{\overline{R}}_i^T .. \overline{\overline{R}}_n^T \end{bmatrix}^T$ and $S = [S_1^T .. S_i^T .. S_n^T]^T$ and calculating the corresponding Moore-Penrose pseudoinverse matrix $\overline{\overline{R}}^{+}$ in such a way that $\overline{\overline{R}}^{+} = (\overline{\overline{R}}^T \cdot \overline{\overline{R}})^{-1} \cdot \overline{\overline{R}}^T$ it is then possible to determine the vector H of the calibration parameters:

$$H = \begin{bmatrix} x_T^{O'} \\ y_T^{O'} \\ z_T^{O'} - \delta \\ a \\ b \\ c \\ \alpha \\ \beta \end{bmatrix} = \overline{\overline{R}}^{+} \cdot S \tag{8}$$

By determining the parameters the calibration procedure can be considered concluded and the scanning system can be independently used to easily measure the coordinates x_{P_k}, y_{P_k} and z'_{P_k} of a generic point k (z'_{P_k} represents the distance along z_f between the point k and an unknown reference plane). This is possible substituting the values of H, d_k, $x_{O'_k}$, $y_{O'_k}$, $z_{O'_k}$, and θ_k into eq (5).

DESCRIPTION OF THE WORKCELL AND DESIGN OF THE SCANNING SYSTEM

The workcell inside which the scanning system performs its measurements is a cell that was conceived for micro scale components manipulation and assembly.

Inside the workcell two manipulators cooperate in different tasks, i.e. peg-in-hole insertions: a 4-dof robot guarantees the positioning of the parts and their orientation around the vertical axis while a 2-dof pointing device (platform) holds and orientate a frame through which the parts are inserted. This solution, even though decoupling the movements of two different mechanisms, ensures the complete mobility of the system and makes the design task much easier, since offering the opportunity to deal with simple kinematic chains [12].

In Fig. 2 the layout of the workcell is displayed.

The assembly task is guaranteed thanks to the presence of one bottom and two top cameras that monitor the presence and position of objects/holes respectively on the center glass plate and on the side aluminum plate and pyramid (this one mounted on the 2-dof orientation platform).

Copyright © 2015 by ASME

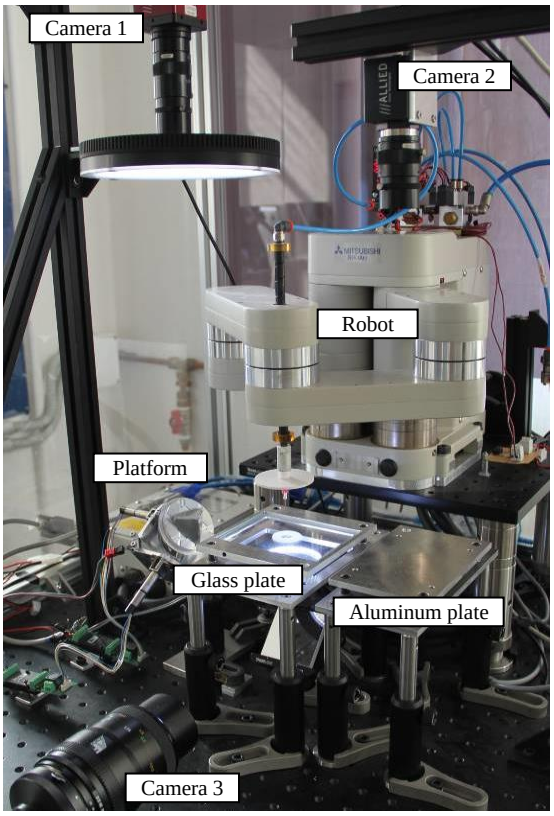

Figure 2. WORKCELL LAYOUT.

All the cameras are previously calibrated and referenced to the fixed frame associated with the manipulator [13].

The generic pick and place movement consists in picking the micro component (standard dimensions between 0.5 and 0.8 mm) from the glass plate by means of a vacuum gripper, lifting it up, dragging it above the pyramid and inserting it inside the corresponding hole.

It is important to draw the attention to the fact that, with some preliminary experiments, it was proved that the manipulator can be considered well calibrated and thus sufficiently accurate to be used together with the cameras for the calibration of other devices (i.e. the orientation platform). It must be said that the availability of this workcell highly conditioned the design and calibration of the scanning system. In particular, the presence of a very accurate 4-dof manipulator and of high performance cameras perfectly matches with the need of a robot able to carry the transducer around and of an external system able to read the coordinates x and y of physical points.

Moreover, the glass plate top surface can act as reference surface since the coordinates x and y of the points lying on it can be easily measured by the bottom camera.

Therefore, it is possible to conclude that, to have a calibration system inside the workcell, the only component missing is the transducer.

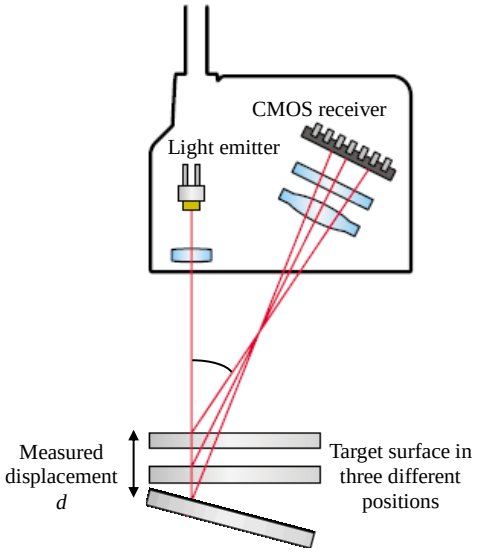

Figure 3. MEASUREMENT PRINCIPLE OF TRIANGULATION SENSORS.

The laser triangulation sensor

After studying the state of the art and examining and comparing different devices already available on the market, the decision to use a commercial high accuracy laser triangulation sensor has been taken.

The description of the chosen high performance laser sensor IL-S065 produced by Keyence is now reported.

These types of laser displacement sensors are composed of a semiconductor light emitter and a CMOS receiver and use the principle of triangulation for measuring movements (Fig. 3). Within a determined range, when the position of the target is altered, the position of the beam spot on the CMOS moves; these devices measure the displacement of the target by detecting the position of the beam spot, regardless of the orientation of the target. The distance is measured with respect to a previously chosen reference point.

The chosen laser sensor [16], presenting 2 μm repeatability and ±0.05% linearity in a 20 mm (±10 mm) measurement range (reference distance = 65 mm), can be considered suitable for the scanning task here proposed.

Moreover, the weight of the scanning head is very low and for this reason it can be carried around by the manipulator without any problem, see Fig. 5. This aspect is essential in any design solution where the laser is meant to be installed at the robot end-effector.

The initialization of the triangulation sensor is obtained by setting to zero the value of the displacement in a chosen configuration within the measurement range. Afterwards, all the values shown on the display of the amplifier unit quantify the displacement, along the preferential direction, of the target surface.

Copyright © 2015 by ASME

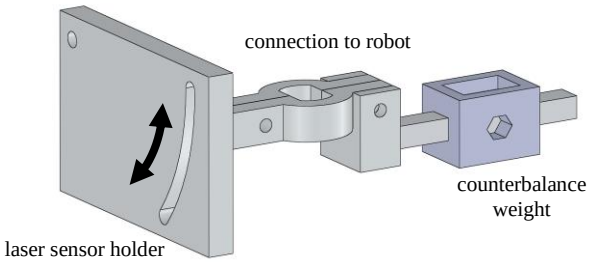

Figure 4. 3D PART OF THE BRACKET.

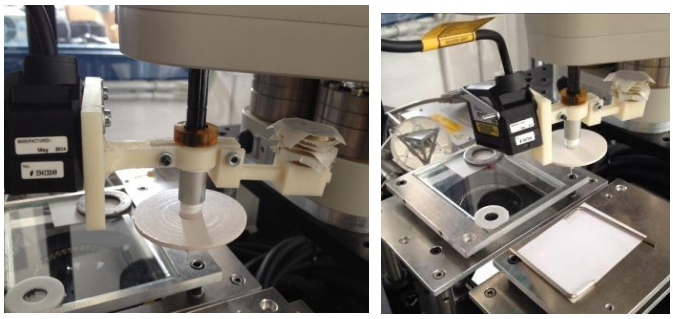

Figure 5. ASSEMBLY OF THE BRACKET AND SENSOR.

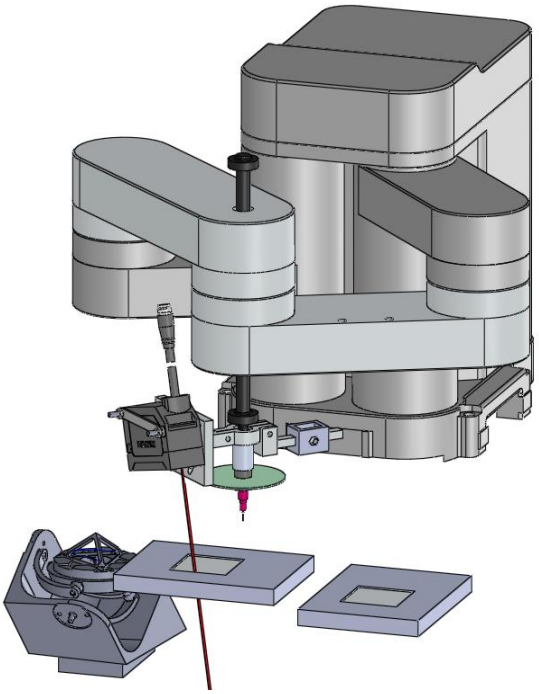

Figure 6. FEASIBILITY STUDY OF THE TASK IN A VIRTUAL ENVIRONMENT.

The mechanical interface

The sensor head has to be mounted on the end-effector of the robot in order to guarantee its full mobility. For this purpose a mechanical interface has been designed and 3D printed (Fig. 4). The aim of this bracket is to rigidly connect the scanning head to the upper part of the end effector.

On one side of the bracket a plate with a hole and a slot ensures the adjustment of the inclination of the laser beam while on the other side a counterbalance weight minimizes the presence of undesirable bending moments along the vertical rod of the robot. Figure 5 shows how the bracket has been fixed to the manipulator.

The horizontal arm of this support, that links the sensor to the gripper, has to be long enough to allow the top cameras to see the laser spot, once the sensor has been sufficiently tilted.

COLLECTION OF DATA: SETUP & IMPLEMENTATION

In order to guarantee the visibility of the laser spot from the cameras in different robot configurations, the layout of the system is reproduced in a virtual environment (see Fig. 6). The two small squares on the top of the glass and aluminum plate identify respectively the fields of view of the bottom and top camera. After some simulations the best position for the top camera has been found.

Moreover, a thin layer of adhesive plastic is applied on the surfaces in order to magnify the contrast between the laser spot and the surrounding area.

The glass surface and the aluminum one are then set approximately horizontal to take into account the reduced depth of field of the vision system.

After a preliminary simulation study, once the layout of the workcell is determined and configured, the calibration procedure can be carried out. The triangulation sensor distance d is first initialized to zero at a generic $z_{O'}$ ($z_{O'}$=20 mm was randomly chosen).

Once the setup is ready, the data related to two xy grids of spots at different constant $z_{O'}$ are acquired. For each point the manipulator controller provides $x_{O'}$, $y_{O'}$, $z_{O'}$ and the rotation angle θ around the z_m axis, the bottom camera measures the spot coordinates x_{Pi} and y_{Pi} and the laser sensor the relative distance d (with respect to the before mentioned zero). All the data now are saved in a text file, imported and handled by the calibration algorithm.

CALIBRATION

After outlining the setup and describing the initialization and the implementation of the data collection, the next step is the calibration of the scanning system, which consists in identifying the laser beam parameters $H = \left(x_T^{O'}, y_T^{O'}, z_T^{O'} - \delta, a, b, c, \alpha, \beta\right)^T$. These parameters are needed for the computation of the laser spot coordinates on a generic surface.

Copyright © 2015 by ASME

Adaptation of the Algorithm

The calibration procedure starts by computing the matrix that describes the rotation of the end-effector with respect to the robot fixed frame. Our robot presents four degrees of freedom, three for the translation along the x_f, y_f and z_f axis, and one for the rotation around the z_f axis. As mentioned before, the coordinates $x_{O'}$, $y_{O'}$ and $z_{O'}$ of the end-effector and its rotation θ around the z_f axis are provided for each configuration i of the robot by its controller, thus the rotation matrix can be computed as hereinafter shown:

$$R_i = \begin{bmatrix} c_{\theta_i} & -s_{\theta_i} & 0 \\ s_{\theta_i} & c_{\theta_i} & 0 \\ 0 & 0 & 1 \end{bmatrix} \tag{9}$$

Moreover, the mathematical algorithm described before can be easily adapted in order to identify the position of the laser beam. Given the angle θ_i, the coordinates $x_{O',i}$, $y_{O',i}$, $z_{O',i}$, the relative distance d_i along the laser beam and the coordinates x_{Pi} and y_{Pi} of the laser spot, substituting all these parameters in (5) the following equation is obtained:

$$\begin{bmatrix} x_{P_i} - x_{O'_i} \\ y_{P_i} - y_{O'_i} \\ z_{P_i} - z_{O'_i} \end{bmatrix}^O = \begin{bmatrix} c_{\theta_i} & -s_{\theta_i} & 0 \\ s_{\theta_i} & c_{\theta_i} & 0 \\ 0 & 0 & 1 \end{bmatrix} \cdot \begin{bmatrix} x_T + a \cdot d_i \\ y_T + b \cdot d_i \\ z_T + c \cdot d_i \end{bmatrix}^{O'} \tag{10}$$

Multiplying the last two matrixes we get:

$$\begin{bmatrix} x_{P_i} - x_{O'_i} \\ y_{P_i} - y_{O'_i} \\ z_{P_i} - z_{O'_i} \end{bmatrix}^O = \begin{bmatrix} x_T \cdot c_{\theta_i} - y_T \cdot s_{\theta_i} + a \cdot d_i \cdot c_{\theta_i} - b \cdot d_i \cdot s_{\theta_i} \\ x_T \cdot s_{\theta_i} + y_T \cdot c_{\theta_i} + a \cdot d_i \cdot s_{\theta_i} + b \cdot d_i \cdot c_{\theta_i} \\ z_T + c \cdot d_i \end{bmatrix}^O \tag{11}$$

Then, following (6) and (7), the matrix $\overline{\overline{R}}_i$ results:

$$\overline{\overline{R}}_i = \left[\begin{array}{ccc|ccc|cc} c_{\theta_i} & -s_{\theta_i} & 0 & d_i \cdot c_{\theta_i} & d_i \cdot s_{\theta_i} & 0 & 0 & 0 \\ s_{\theta_i} & c_{\theta_i} & 0 & d_i \cdot s_{\theta_i} & d_i \cdot c_{\theta_i} & 0 & 0 & 0 \\ 0 & 0 & 1 & 0 & 0 & d_i & -x_{p_i} & -y_{p_i} \end{array}\right] \tag{12}$$

Overall, during the data acquisition, three grids of points, with the robot having the same angle θ but different heights, are collected. An additional set of points is also collected by varying the rotation of the end-effector.

All these data, related to n different configurations of the scanning system, are substituted into (7) and arranged in one equation, as shown below:

$$\begin{bmatrix} x_{P_1} - x_{O'_1} \\ y_{P_1} - y_{O'_1} \\ -z_{O'_1} \\ \vdots \\ x_{P_n} - x_{O'_n} \\ y_{P_n} - y_{O'_n} \\ -z_{O'_n} \end{bmatrix}^O = \begin{bmatrix} \overline{\overline{R}}_1 \\ \dots \\ \overline{\overline{R}}_n \end{bmatrix} \cdot H \tag{13}$$

which is finally solved as (8)

$$H = \overline{\overline{R}}^{+} \cdot S \tag{14}$$

Preliminary Results

During the experimental campaign 42 points on the glass plane have been considered and the calibration process, within about 30 minutes, just the time to move the robot to the different poses, has identified the following parameters:

$$H = \begin{bmatrix} x_T^{O'} \\ y_T^{O'} \\ z_T^O - \delta \\ a \\ b \\ c \\ \alpha \\ \beta \end{bmatrix} = \begin{bmatrix} -6.386\,[mm] \\ 70.055\,[mm] \\ -20.073\,[mm] \\ 0.250 \\ -0.181 \\ 0.952 \\ -0.713 \times 10^{-3} \\ 5.671 \times 10^{-3} \end{bmatrix} \tag{15}$$

As shown in (15), in our specific case $z_T^{O'}$ can be substituted with z_T^O since the rotation R is always performed around the z_f axis.

Once the laser beam parameters are obtained, a first test to assess the precision of the results is the verification of the relationship $a^2+b^2+c^2=1$ that in this case is well respected ($a^2+b^2+c^2=1.001131$).

Moreover, there is another way to assess the accuracy of the calibration algorithm. If the coordinates x_P, y_P and z_P-z_T of the points are computed by modifying equation (5) as follows

$$\begin{bmatrix} x_P \\ y_P \\ z_P - z_T \end{bmatrix}^O = R \cdot \begin{bmatrix} x_T + a \cdot d \\ y_T + b \cdot d \\ c \cdot d \end{bmatrix}^{O'} + \begin{bmatrix} x_{O'} \\ y_{O'} \\ z_{O'} \end{bmatrix}^O \tag{16}$$

x_P and y_P can be compared with the coordinates provided by the camera and the obtained differences can be used to quantify the errors introduced by adopting the described method.

Copyright © 2015 by ASME

Table 1. ERRORS INTRODUCED WITH THE SCANNING SYSTEM.

Coordinate	Mean absolute error [mm]	Mean square error [mm]	Maximum error [mm]
x	0.017	0.020	0.041
y	0.012	0.016	0.038
z	0.009	0.012	0.038

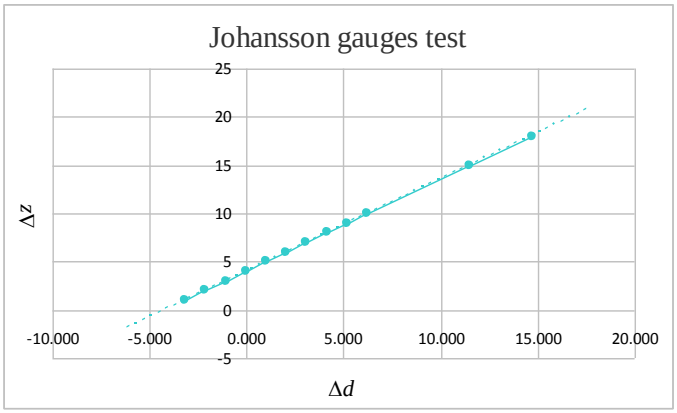

Figure 7. JOHANSSON GAUGES TEST - LEAST SQUARE LINE OF BEST FIT.

Similarly, since the considered plane is nearly horizontal, the error on z can be estimated by comparing the $z_{O'}$ given by the manipulator with the one computed after substituting the camera coordinate into (7).

These errors are summarized in Tab. 1 and displayed in Fig. 8. Figure 8 confirms that, once the scanning system is calibrated, the algorithm can compute the coordinates of the scanned points with really high precision. The inaccuracy in the manipulator movements affects the errors on all the *xyz* coordinates, while the inaccuracy of the cameras mainly affects the *xy* errors, and the inaccuracy of the laser sensors mainly affects the error on z since the laser beam is nearly parallel to z axis. Data about the resolution and errors of the calibrated cameras and the repeatability of the 4-dof manipulator are reported in Tab. 2.

A further test has been performed by using Johansson gauges. Once the system is calibrated a number of different gauges can be placed on the plane in such a way that the laser spot hits them.

Since each gauge has a very well known size Δz, a least square analysis of the different Δz and of the corresponding Δd read by the sensor permits to estimate the constant c of vector H. Performing this task c=0.954 has been obtained, which match very well with the results of eq. (15), see Fig. 7.

APPLICATIONS FOR THE SCANNINNG SYSTEM

Hereinafter, examples of applications for the scanning system are reported. All of them are based on the ability of the system to determine the coordinates of a point.

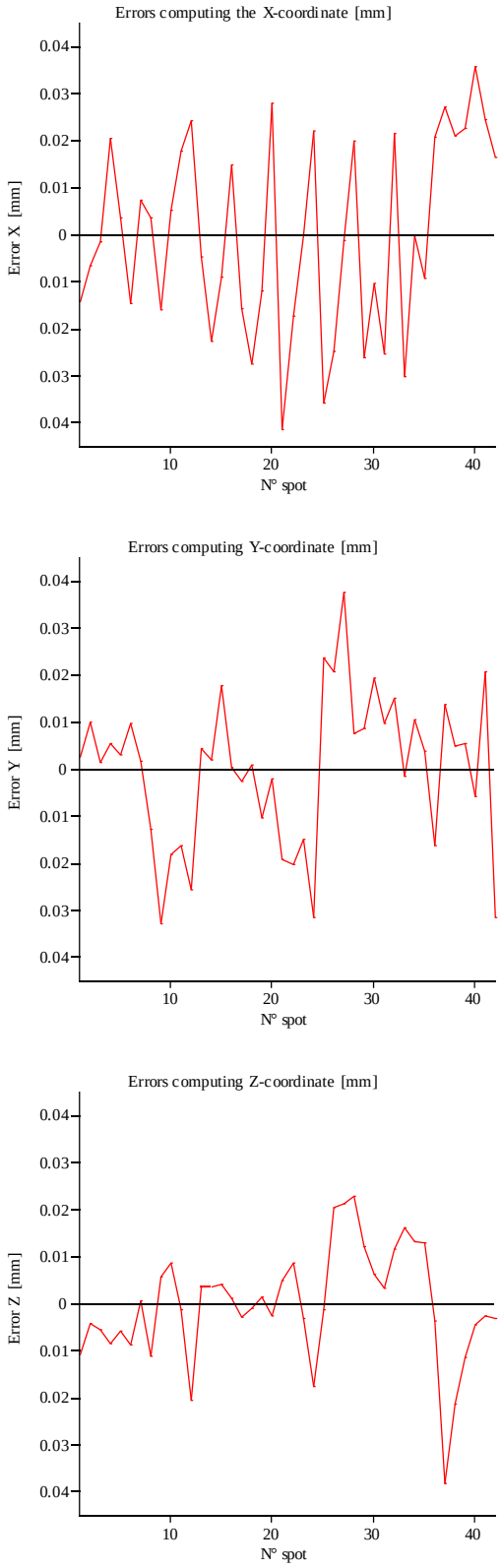

Figure 8. ERRORS INTRODUCED COMPUTING THE POINT COORDINATES.

Copyright © 2015 by ASME

Table 2. RESOLUTION AND ERRORS OF THE CALIBRATED CAMERAS AND REPEATABILITY OF THE 4-DOF MANIPULATOR.

Camera	Spatial resolut. [μm]	Mean error [μm]	Maximum error [μm]	Standard dev. [μm]
Bottom (glass plate)	6.6	6.3	19.0	3.1
Top (aluminum plate)	24.0	19.5	46.2	12.3

	Movements on the x-y plane [μm]	Vertical motion [μm]	End-effector rotation [°]
Manipulator Repeatability	±5	±10	±0.02

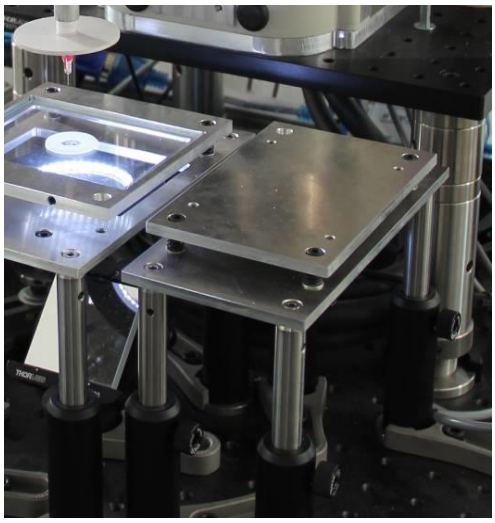

Figure 9. ALUMINUM PLATE USED TO VALIDATE THE SCANNING SYSTEM.

Identification of a plane

A first application of the laser measuring device is the identification of a plane.

In order to test the precision of the measuring system when operating in an area far from where it was calibrated, the following test has been performed.

The scanning system has been used to scan the aluminum plate located next to the glass plate, see Fig. 9. The robot has been moved to different $xyz\theta$ coordinates and the distance d has been measured by the laser sensor. For each pose the xyz coordinates of the laser spot have been estimated by equation (16). Since the points identified by the laser beam lay on a plane, this plane can be estimated with the least square criteria.

Following the procedure, a plane can be described with respect to the absolute reference system by the following equation:

$$z_{P_i} - z_T = \alpha \cdot x_{P_i} + \beta \cdot y_{P_i} - (z_T - \delta) \qquad (17)$$

Collecting a number h of points P_i that belong to the same plane, from the equation (17), for each point i, we get:

Table 3. ERROR ESTIMATES FOR THE PLANE PARAMETERS.

Parameter	Data from scanning system	Data from top camera	Error estimate
α	4.152 x10^{-3}	4.154 x10^{-3}	2.045 x10^{-6}
β	-3.153 x10^{-3}	-3.168 x10^{-3}	-1.519 x10^{-5}
$z_T - \delta$ [mm]	-14.981	-14.982	-1.217 x10^{-3}

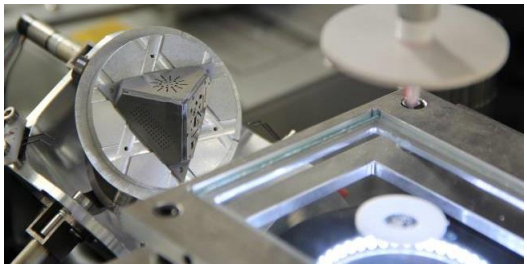

Figure 10. 2-DOF ORIENTATION PLATFORM THAT IS GOING TO BE CALIBRATED.

$$z_{P_i} - z_T = \begin{bmatrix} x_{P_i} & y_{P_i} & -1 \end{bmatrix} \cdot \begin{bmatrix} \alpha \\ \beta \\ z_T - \delta \end{bmatrix} = L_i \cdot \begin{bmatrix} \alpha \\ \beta \\ z_T - \delta \end{bmatrix} \qquad (18)$$

Therefore, considering the coordinates of all the points h:

$$\begin{bmatrix} z_{P_1} - z_T \\ \vdots \\ z_{P_h} - z_T \end{bmatrix} = \begin{bmatrix} x_{P_1} & y_{P_1} & -1 \\ \vdots & & \\ x_{P_h} & y_{P_h} & -1 \end{bmatrix} \cdot \begin{bmatrix} \alpha \\ \beta \\ z_T - \delta \end{bmatrix} = \bar{L} \cdot \begin{bmatrix} \alpha \\ \beta \\ z_T - \delta \end{bmatrix} \qquad (19)$$

By adopting the method of the least squares it is then possible to determine the parameters α, β and $z_T - \delta$ of the plane:

$$\begin{bmatrix} \alpha \\ \beta \\ z_T - \delta \end{bmatrix} = \left(\bar{L}^T \cdot \bar{L} \right)^{-1} \cdot \bar{L}^T \cdot \begin{bmatrix} z_{P_1} - z_T \\ \vdots \\ z_{P_h} - z_T \end{bmatrix} \qquad (20)$$

that, for the aluminum plate, are reported on the first column of Tab. 3.

Comparing these values with the ones obtained substituting the coordinates of the points acquired by the already calibrated top camera into (14), it is possible to estimate the errors on the workplane parameters, as shown in Tab. 3. Moreover, the estimated values of the xy coordinates of the single spot can also be compared with the ones acquired by the camera, while the estimated value of the z coordinate can be compared with the one obtained by inserting the xy coordinates measured by the same camera into (17). The results of the comparison are reported in Tab. 4 and in Fig. 12 and a description of the camera system and of its calibration is available in [15].

Copyright © 2015 by ASME

Table 4. ERRORS OF THE POINT COORDINATES ON THE SIDE PLATE.

Coordinate	Mean absolute error [mm]	Mean square error [mm]	Maximum error [mm]
x	0.031	0.090	0.041
y	0.054	0.178	0.069
z	0.054	0.128	0.065

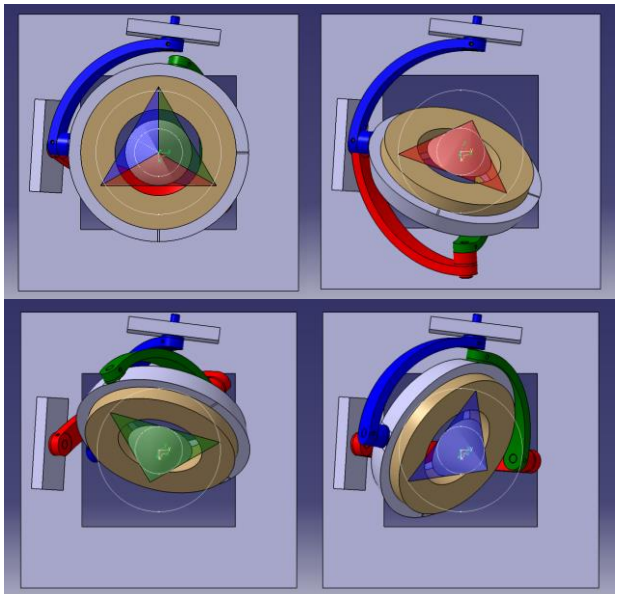

Figure 11. DIFFERENT POSES OF THE ORIENTATION PLATFORM HOLDING THE PIRAMID [17].

Calibration of a robot

As stated at the beginning of this work, the scanning device has been conceived to perform mini robot calibration tasks. The robot to be calibrated is the two dof orientation platform of Fig. 10 and 11, described in [17]; this is a 2-dof version of the agile-eye [18]. If the platform is moved to some different poses and in each of them the pyramid pose is measured by the scanning system, it is possible to reconstruct its real kinematics by applying standard calibration procedure [2, 3, 4, 19].

The measurement of the pyramid pose may be performed by identifying the 3 faces and, on each of them, carrying out the task just described for one plane. In particular, to get the pyramid pose it is necessary to identify at least 3 points on each face and estimate the equation of the related plane. By intersecting the three planes the coordinates of the apex of the pyramid and the unit vectors collinear to the edges are found. In this way it is possible to obtain the position and orientation of the platform and, by means of the already developed system of parametric equations in 19 parameters, perform the calibration.

The results of this study are not available yet, but it is aim of the authors to accomplish this task in the near future as final step of the research.

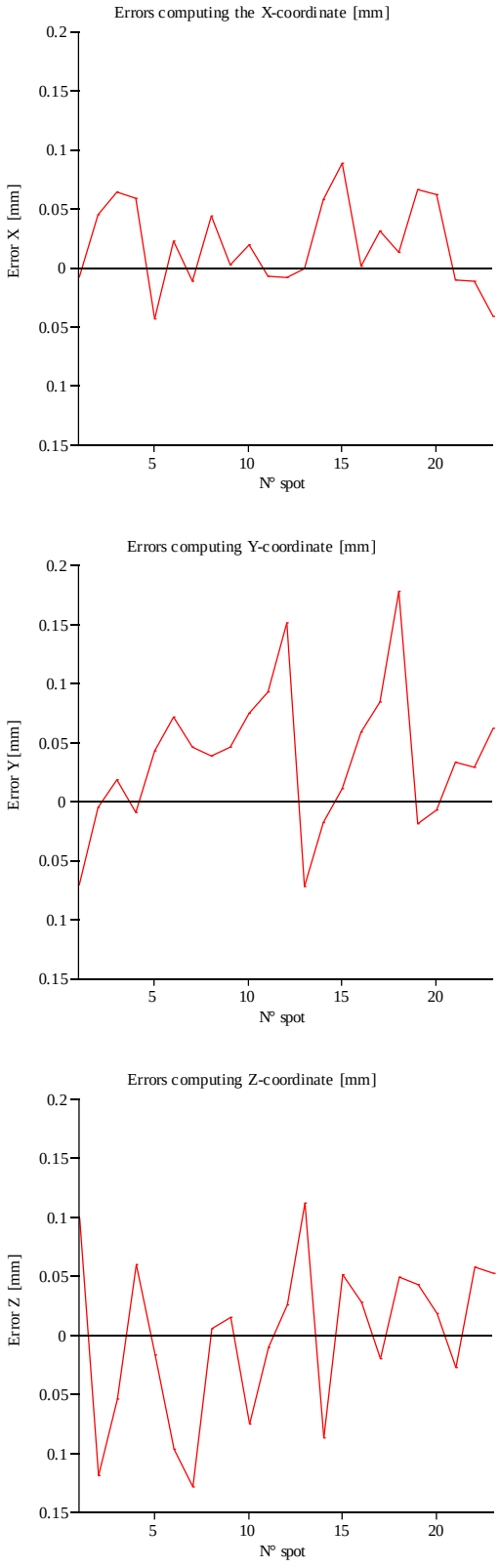

Figure 12. ERRORS INTRODUCED ESTIMATING THE POINT COORDINATES WITH THE SCANNING SYSTEM.

Copyright © 2015 by ASME

CONCLUSIONS

The need, within the project PRIN2009, of quantifying the accuracy of an already prototyped 2-dof orientation platform in order to perform micro assembly and manipulation tasks inside an existing working cell brought the idea of designing a new calibration system. This system is able to acquire coordinates of points by scanning surfaces. The laser calibration device, described in this paper, is presented as an innovative instrument that could be used in a variety of applications. In particular, it would be very useful for the identification of the pose of different objects and also for the calibration of mini robots. In fact, as proved in this work, it can be implemented in automatized tasks without risk to lose in accuracy. After describing the steps followed in the design of the device and in the development of the mathematical algorithm, some results of the experiments conducted in the work cell for the calibration of the scanning system have been reported. They demonstrate the reliability of the system, whenever used to identify the point coordinates, that can be quantified in a maximum mean square error value equal to 0.03 mm. In conclusion, considered the positive results obtained, it is possible to say that the use of the device, first to describe the pose of the mentioned orientation platform and then to calibrate it, can represent the next step of the authors' research study.

ACKNOWLEDGMENTS

Work partially supported by project PRIN2009 MM&A Micro Manipulation and Assembly, funded by MIUR Italian Minister for Higher Education.

REFERENCES

[1] ISO 9283:1998, Manipulating industrial robots - Performance criteria and related test methods.

[2] Mooring, B., Roth, Z. S. and Driels, M. R., 1991. "Fundamentals of manipulator calibration", Journal of Robotic Systems Wiley.

[3] Legnani, G., Omodei, A. and Adamini, R., 2000. "Three Methodologies for the calibration of Industrial Manipulators: Experimental Results on SCARA Robot". Journal Of Robotics System, 17(6), pp 291-307.

[4] Legnani, G., Tiboni, M., Adamini, R.and Tosi, D., 2009. "An Innovative Neural Network based approach for the kinematics calibration of industrial robots", 18th Int. Workshop on RAAD2009 - Robotics in Alpe-Adria-Danube Region, Brasov, Romania, May, pp. 25-27.

[5] ISO/TR 13309:1995, Manipulating industrial robots - Informative guide on test equipment and metrology methods of operation for robot performance evaluation in accordance with ISO 9283.

[6] Legnani, G. and Tiboni, M., 2014. "Optimal Design And Application of a Lowcost Wire-Sensor System for the Kinematic Calibration of Industrial Manipulators. Mechanism And Machine Theory", Vol. **73**, pp. 25–48. ISSN:0094-114X.

[7] Ye, C. and Borenstein, J., 2002. "Characterization of a 2-D Laser Scanner for Mobile Robot Obstacle Negotiation". Proceedings of the 2002 IEEE International Conference on Robotics and Automation. Washington DC, USA, 10-17 May, pp. 2512-2518.

[8] Leica Geosystems, URL http://www.leica-geosystems.it/it/Laser-Scanner-HDS_5570.

[9] Tsai, R. Y. and Lenz, R. K., 1989 "A New Technique for Fully Autonomous and Efficient 3D Robotics Hand/Eye Calibration", IEEE Transactions on Robotics and Automation, Vol. **5**, No.3, pp.345–358.

[10] Chen, H. 1991. "A Screw Motion Approach to Uniqueness Analysis of Head-Eye Geometry". In Proceedings of Computer Vision and Pattern Recognition (CVPR), Maui, Hawaii, IEEE Computer Society Press, pp. 145–151.

[11] Fassi, I. and Legnani, G., 2005. "Hand to Sensor Calibration: a Geometrical Interpretation of the Matrix Equation AX=XB", Journal of Robotic Systems, 22(9), pp 497-506.

[12] Fontana, G., Ruggeri, S, Fassi, I.and Legnani, G., 2014. "A mini work-cell for handling and assembling microcomponents, assembly". Automation Journal, Emerald.

[13] Ruggeri, S., Fontana, G., Pagano, C., Fassi, I. and Legnani, G., 2012. "Handling and Manipulation of Microcomponents: Work-Cell Design and Preliminary Experiments". in Proc. of International Precision Assembly Seminar IPAS 2012, Chamonix, France, 12-15 February, pp. 65-72.

[14] Lee, C.-C. and Hervé, J. M., 2011. "Isoconstrained Parallel Generators of Schoenflies Motion". J. Mechanisms Robotics, 3(2), March, DOI:10.1115/1.4003690.

[15] Fontana, G., Ruggeri, S., Fassi, I. and Legnani, G., 2013. "Flexible vision based control for micro-factories", in Proc. of 7th Int. Conference on Micro- and Nanosystems IDETC/MNS 2013, Portland, OR, USA, August, pp. 4-7.

[16] Keyence Corporation, URL http://www.keyence.com/.

[17] Palmieri, G.; Callegari, M.; Carbonari, L. and Palpacelli, M.C., 2014. "Design and testing of a spherical parallel mini manipulator". In Proc. 10th International on Mechatronic and Embedded Systems and Applications (MESA), IEEE/ASME, pp. 1–6. DOI:10.1109/ MESA.2014.6935523. Print ISBN: 978-1-4799-2772-2.

[18] Gosselin, C., St.Pierre, E. and Gagne, M., 1996. "On the development of the Agile Eye". Robotics & Automation Magazine, IEEE, Vol. **3**, Issue 4, pp. 29-37, ISSN: 1070-9932, DOI: 10.1109/100.556480.

[19] Omodei, A., Legnani, G. and Adamini, R.,"Calibration of a Measuring Robot: Experimental Results on a 5 DOF Structure". Journal of Robotic Systems. Wiley, Vol.18, N.5, May, pp. 237-250.

 Copyright © 2015 by ASME